

## Article

# Where ppm Quantities of Silsesquioxanes Make a Difference—Silanes and Cage Siloxanes as TiO<sub>2</sub> Dispersants and Stabilizers for Pigmented Epoxy Resins

Dariusz Brząkałski <sup>1</sup>, Robert E. Przekop <sup>2,\*</sup>, Miłosz Frydrych <sup>1</sup>, Daria Pakuła <sup>1</sup>, Marta Dobrosielska <sup>3</sup>, Bogna Sztorch <sup>2</sup> and Bogdan Marciniak <sup>1,2,\*</sup>

<sup>1</sup> Faculty of Chemistry, Adam Mickiewicz University in Poznań, 8 Uniwersytetu Poznańskiego, 61-614 Poznań, Poland; d.brzakalski@gmail.com (D.B.); frydrych@amu.edu.pl (M.F.); darpak@amu.edu.pl (D.P.)

<sup>2</sup> Centre for Advanced Technologies, Adam Mickiewicz University in Poznań, 10 Uniwersytetu Poznańskiego, 61-614 Poznań, Poland; bogna.sztorch@amu.edu.pl

<sup>3</sup> Faculty of Materials Science and Engineering, Warsaw University of Technology, 141 Wołoska, 02-507 Warsaw, Poland; Marta.Dobrosielska@pw.edu.pl

\* Correspondence: r.przekop@gmail.com or rprzekop@amu.edu.pl (R.E.P.); bogdan.marciniak@amu.edu.pl (B.M.)



**Citation:** Brząkałski, D.; Przekop, R.E.; Frydrych, M.; Pakuła, D.; Dobrosielska, M.; Sztorch, B.; Marciniak, B. Where ppm Quantities of Silsesquioxanes Make a Difference—Silanes and Cage Siloxanes as TiO<sub>2</sub> Dispersants and Stabilizers for Pigmented Epoxy Resins. *Materials* **2022**, *15*, 494. <https://doi.org/10.3390/ma15020494>

Academic Editors: Alessandro Pegoretti, Rani F El Elhajjar and Milena Pavlíková

Received: 10 November 2021

Accepted: 5 January 2022

Published: 10 January 2022

**Publisher's Note:** MDPI stays neutral with regard to jurisdictional claims in published maps and institutional affiliations.



**Copyright:** © 2022 by the authors. Licensee MDPI, Basel, Switzerland. This article is an open access article distributed under the terms and conditions of the Creative Commons Attribution (CC BY) license (<https://creativecommons.org/licenses/by/4.0/>).

**Abstract:** In this work, silsesquioxane and spherosilicate compounds were assessed as novel organosilicon coupling agents for surface modification of TiO<sub>2</sub> in a green process, and compared with their conventional silane counterparts. The surface-treated TiO<sub>2</sub> particles were then applied in preparation of epoxy (EP) composites and the aspects of pigment dispersion, suspension stability, hiding power, as well as the composite mechanical and thermal properties were discussed. The studied compounds loading was between 0.005–0.015% (50–150 ppm) in respect to the bulk composite mass and resulted in increase of suspension stability and hiding power by over an order of magnitude. It was found that these compounds may be an effective alternative for silane coupling agents, yet due to their low cost and simplicity of production and manipulation, silanes and siloxanes are still the most straight-forward options available. Nonetheless, the obtained findings might encourage tuning of silsesquioxane compounds structure and probably process itself if implementation of these novel organosilicon compounds as surface treatment agents is sought for special applications, e.g., high performance coating systems.

**Keywords:** silsesquioxane; spherosilicate; cage siloxane; silane; POSS; composite; titanium white; coating; surface treatment; coupling agent

## 1. Introduction

In polymers industry, additives are applied to fulfil one or more of multiple tasks at once: to cut costs (extending fillers, mostly), to improve mechanical properties (plasticizers, reinforcing fillers, e.g., fibres, nanoparticles), to reduce flammability (fire retardants), to improve the processability for the given processing technology or the final surface properties (lubricants, defoamers), or to add colour to the material (pigments). For inorganic additives, their price is one of the main decisive factors behind considering a given additive both an extending filler and a special purpose additive (functional filler), or just the latter [1,2]. The more expensive additives need to be applied in reasonable quantities in order to keep the production of the desired material economically viable. In case of pigments, there are more and less economical options available, differing also in terms of pigmentation efficiency and environmental friendliness. Regarding white pigments, the most commonly used white pigment is titanium white (TiO<sub>2</sub>), characterized by high pigmentation efficiency thanks to its nanostructure and quite good dispersibility, and comprising 69% of the worldwide market of inorganic pigments in year 2000, and together with carbon black

and iron oxides, for over 90% of the world market in 2009 [3,4]. At the same time, titanium white is relatively expensive (around 2500 EUR as of 2020 [5]). Although being an effective pigment, it naturally agglomerates in polymer matrix, which results in need for using it at higher loadings, especially in thin foils, to achieve the desired opacity/pigmentation. Therefore, achieving good dispersion of TiO<sub>2</sub> within polymer translates to reduction of the amount of the pigment used, while obtaining the same pigmentation level and thus reducing the production price for the given plastic material, as well as saving the natural resources used. Titanium white is not considered a high performance pigment due to its cost and agglomeration tendency, therefore treatment procedures are applied in industry and being studied in R&D [3,4].

Epoxy resins are available on the market in different colours for two main reasons. The first one is obviously the aesthetic value, as they are often used for decoration/artistic purposes. Secondly, epoxy resins are commonly slightly yellow in colour, and even more often are the curing components (hardeners) thereof, especially the most common amine type ones. Upon storage, this yellow colour becomes more intense. Therefore, colouration/pigmentation of the epoxy allows to hide this discolouration and make the resin colour more reproducible from batch to batch during production. In case of storing the resin, it is important for the pigment to form a stable mixture with the epoxy base and not to separate from it upon time. Therefore, white-pigmented epoxy resins of satisfactory shelf-life are of high demand and increasing this shelf-life is sought [4,6]. Also, improved dispersion translates into increased hiding power, understood as the coating ability of optically blocking the surface it covers [7].

Organosilicon compounds are nowadays the most common agents for surface treatment of inorganic materials, the older and discontinued agents being chromium and titanium-based [8,9]. For over 20 years now, silsesquioxane derivatives have been studied as a novel class of organosilicon compounds suitable as polymer processing additives. In comparison to traditional silane coupling agents, their polarity, melting temperatures and vapour pressures are much lower, allowing them to be directly processed with a polymer, which is strongly limited for organofunctional silanes. Also, for a couple of years now, silsesquioxanes have been studied as a new class of silane coupling agents for treatment of inorganic fillers and other particles/nanoparticles. In terms of serving as direct polymer additives for epoxy resins, silsesquioxane compounds were introduced both in a reactive and non-reactive (physical blending) manner. For reactive additives, *i*Oc<sub>7</sub>SSQ-(CH<sub>2</sub>)<sub>3</sub>NH<sub>2</sub> [10], *i*Bu<sub>7</sub>SSQ-(CH<sub>2</sub>)<sub>3</sub>NH<sub>2</sub> [11], 3-glycidoxypropylhepta(isobutyl)octasilsesquioxane [12], 3-glycidoxypropylhepta(isooctyl)octasilsesquioxane and 3-glycidoxypropylheptaphenyloctasilsesquioxane [13] epoxy cyclohexylhepta(isobutyl)octasilsesquioxane [14], (3-glycidoxypropyl)silsesquioxane cage mix [14,15], tris(glycidyl dimethylsiloxy)hepta(isobutyl)silsesquioxane [16,17], octakis(aminophenyl)octasilsesquioxane [18], octakis(3-aminopropyl)octasilsesquioxane [19] mixed substituent hexyl/4-glycidylbutyloctaspherosilicates [13], and hybrids of DGEBA with SSQ molecules attached as a side group [13]. For non-reactive additives, Ph<sub>7</sub>SSQ-3OH (phenyltrisilanol) and *i*Bu<sub>7</sub>SSQ-3OH (isobutyltrisilanol) [20], 9,10-dihydro-9-oxa-10-phosphaphenanthrene-10-oxide (DOPO)-modified silsesquioxanes [21], methyl- and methyl-vinyl polysilsesquioxanes [22] were used. Additionally, in recent years, green chemical approach towards preparation of hybrid materials is sought and the examples of the first silsesquioxane-containing materials prepared in aqueous conditions were given [23]. Silsesquioxanes, as well as polysilsesquioxanes, have been studied as additives moderating dielectric properties of nanocomposites and nanocomposite films [24].

For improved dispersion and interaction with the matrix polymer, TiO<sub>2</sub> has been treated with Ph<sub>7</sub>SSQ-3OH [25,26] and *i*Bu<sub>7</sub>SSQ-3OH [27,28], for processing of polyolefin nanocomposites; *i*Bu<sub>7</sub>SSQ-(CH<sub>2</sub>)<sub>3</sub>NH<sub>2</sub> (for preparation of hybrid graphene oxide-TiO<sub>2</sub> material and cyanate ester composite containing thereof [29]), as to verify these compounds as novel coupling agents for surface treatment of inorganic nanoparticles.

In this work, an approach towards application of well-defined organosilicon compounds, that is, silsesquioxane and spherosilicate derivatives, as dispersants and stabilizers

of TiO<sub>2</sub> nano- and microparticles is presented. More importantly, they were used at low loadings for the studied solution to be economically viable, as well as technologically feasible during standard procedures of pigment manufacturing or pigmented epoxy preparation, without no additional chemical processing steps or organic solvents involved during surface treatment. The organosilicon compounds are compared to much cheaper and readily available, conventional silane coupling agents (trialkoxysilanes) to assess any possible advantages of the former.

## 2. Materials and Methods

### 2.1. Materials and Instrumentation

The chemicals were purchased from the following sources: Tetraethoxysilane (TEOS), tetrachlorosilane, chlorodimethylsilane, tetramethylammonium hydroxide (TMAH) 25% methanol solution from ABCR, *isobutyltrimethoxysilane*, triethylamine, allyl-glycidyl ether, vinyltrimethoxysilane, chloroform-*d* and Karstedt's catalyst xylene solution from Aldrich, P<sub>2</sub>O<sub>5</sub>, tetrahydrofuran (THF), methanol, hydrochloric acid, toluene, acetonitrile, and acetone from Avantor (Poland). Toluene was degassed and dried by distilling it from P<sub>2</sub>O<sub>5</sub> under argon atmosphere. TiO<sub>2</sub> was obtained from Grupa Azoty Z.Ch. "Police" S.A. (Poland), as a 50% *w/w* water slurry with no additives. Epidian 5 was obtained from Ciech Sarzyna (Poland) and according to the manufacturer's data, was characterized by density of 1.17 g/cm<sup>3</sup> and viscosity of 20,000–30,000 mPa·s at 25 °C, and epoxide number of 0.48–0.51 mol/100 g. Curing agent, triethylenetetramine (branded as Z-1 hardener), was also purchased from Ciech.

Octahydrospherosilicate was prepared according to a literature procedure [30]. Chlorohepta(*isobutyl*)octasilsesquioxane was prepared according to literature procedures [31,32]. <sup>1</sup>H, <sup>13</sup>C, and <sup>29</sup>Si Nuclear Magnetic Resonance (NMR) spectra were recorded at 25 °C on a Bruker Ascend 400 and Ultra Shield 300 spectrometers using CDCl<sub>3</sub> as a solvent. Chemical shifts are reported in ppm with reference to the residual solvent (CHCl<sub>3</sub>) peaks for <sup>1</sup>H and <sup>13</sup>C.

Fourier Transform-Infrared (FT-IR) spectra were recorded on a Nicolet iS 50 Fourier transform spectrophotometer (Thermo Fisher Scientific) equipped with a diamond ATR unit with a resolution of 0.09 cm<sup>-1</sup>.

Differential scanning calorimetry (DSC) was performed using a NETZSCH 204 F1 Phoenix calorimeter. Samples of 6 ± 0.2 mg were placed in an aluminium crucible with a punctured lid. The measurements were performed under nitrogen in the temperature range of –30–230 °C and at a 5 °C/min heating rate. T<sub>gu</sub> was measured from the first heating cycle, T<sub>g</sub> was measured from the second heating cycle.

MALDI-TOF mass spectra were recorded on a UltrafleXtreme mass spectrometer (Bruker Daltonics), equipped with a SmartBeam II laser (355 nm) in the 500–4000 *m/z* range. 2,5-Dihydroxybenzoic acid (DHB, Bruker Daltonics, Bremen, Germany) served as matrix. Mass spectra were measured in reflection mode. The data were analysed using the software provided with the Ultraflex instrument—FlexAnalysis (version 3.4).

SEM/EDS analyses were recorded on a Quanta FEG 250 (FEI) instrument; SEM at 5 kV and EDS at 30 kV, respectively. The samples were frozen in liquid nitrogen and fractured with pliers to reveal satisfactory surface for analysis.

Rheological measurements were performed on Anton Paar MCR302 dynamic mechanical thermal (DMTA) rheometer, working in plate-plate configuration, using 25 mm plates.

Contact angle analyses were performed by the sessile drop technique at room temperature and atmospheric pressure, with a Krüss DSA100 goniometer. Three independent measurements were performed for each sample, each with a 5 µL water drop, and the obtained results were averaged to reduce the impact of surface nonuniformity.

For tensile and flexural strength tests, a Universal testing machine Instron 5969 was used, in accordance to the norm EN ISO 527-2:1996. The speed of traverse was set to 2 mm/min for both tensile strength and flexural strength tests.

The measurements of hiding power were performed by placing the samples of prepared resin systems in the optical path between the light source (an LED) and a UV-NIR spectrophotometer, AvaSpec-Mini2048CL (Avantes, Louisville, CO, USA). The amount of light transmitted through the sample was measured and on this basis, the relative hiding strength was determined, 1Ti(s) sample being used as a reference of the lowest value.

For mixing of base epoxy resin with  $\text{TiO}_2$ , a self-made mixing device was used (see Supplementary Information, Figure S1). The machine was based on a high-torque Internal gear (Crescent type, Figure 1) rotary positive displacement pump (Yildiz Pompa YKF 1, Turkey) powered by a 0.75 kW electrical engine (Marelli Motori D6C 90 S6 B3, Italy). The setup was characterized by 900 rpm of maximum operating speed. The pump was connected to a reservoir in a closed circuit setup, resulting in constant circulation of the resin under high shear stress, inflicting mechanical breakdown of  $\text{TiO}_2$  particles and improved dispersion of  $\text{TiO}_2$  within the epoxy resin. During the mixing cycle, the resin would heat up to  $\sim 45^\circ\text{C}$  due to internal friction, which resulted in a significant viscosity drop (as simulated by DMTA analysis under constant shear and temperature gradient conditions, presented in Figure 2), which additionally helped with nanoparticle dispersion.

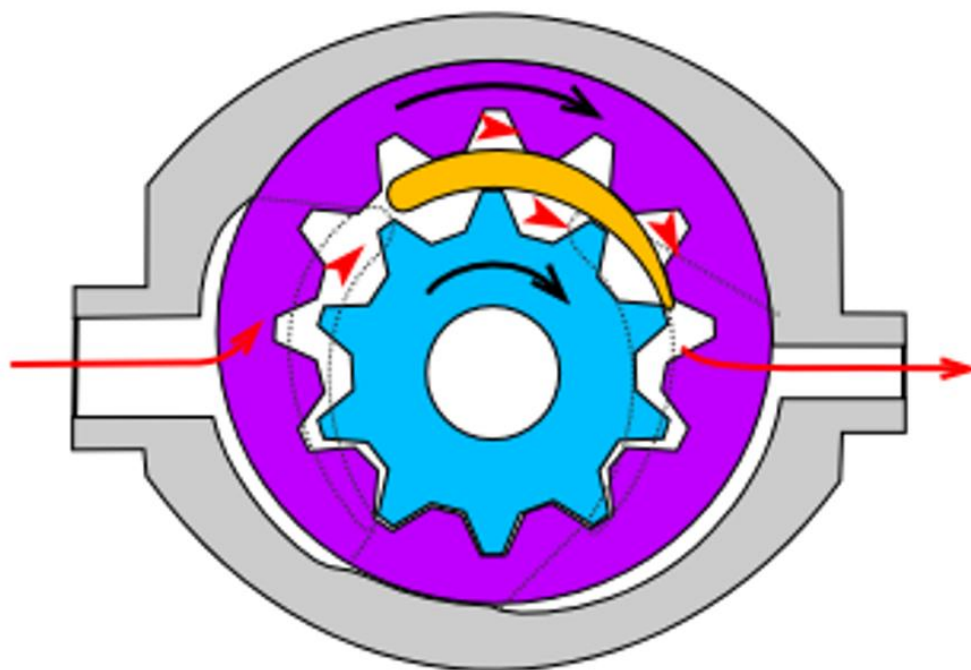


**Figure 1.** Internal gear pump (crescent type) design scheme. Red arrows present the pathway of the pumped medium, the black ones—the rotation direction of the gears. Source: <https://commons.wikimedia.org/w/index.php?curid=38795>, Creative Commons license CC BY-SA 3.0. Accessed on 2 September 2021.

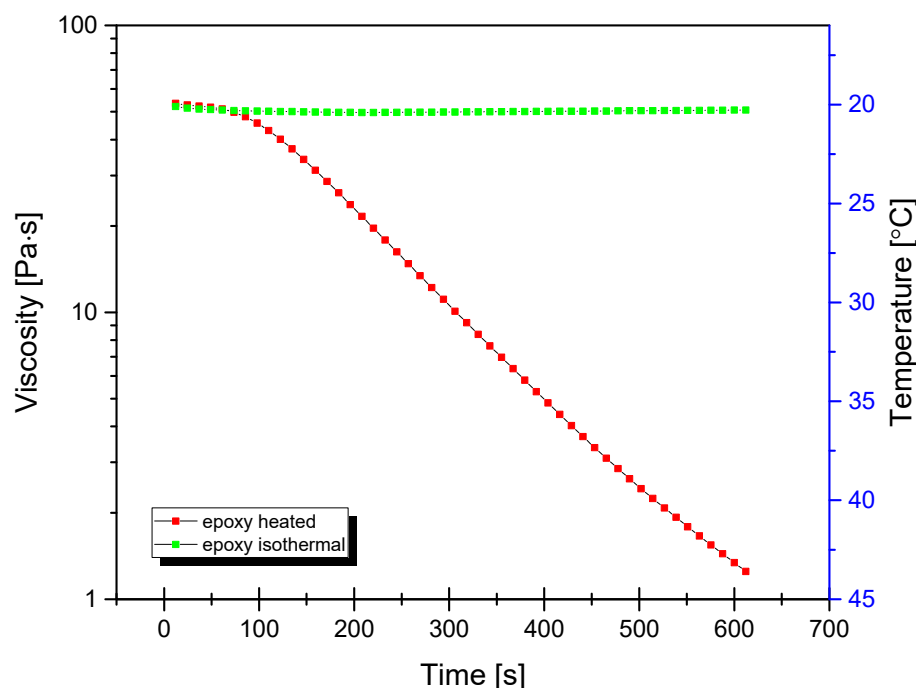


**Figure 2.** Dynamic viscosity curves of neat epoxy under isothermal and non-isothermal conditions under constant shear rate of 100/s.

### 2.2. Procedure for Hydrosilylation of Octaspherosilicates

All hydrosilylation syntheses were conducted under argon atmosphere in round-bottom flasks equipped with condensers, gas bubblers, and magnetic stirrers, the general approach being reported earlier [33]. In a typical procedure, a 500 mL three-neck, round-bottom flask was charged with 25 g of octahydrospherosilicate, 250 mL of dry toluene and a mixture of olefins (allyl-glycidyl ether and vinyltrimethoxysilane, 6:2 molar ratio for SS-6GP-2TMOS, 5:3 ratio for SS-5GP-3TMOS). A thermometer and condenser equipped with an argon inlet and oil bubbler were attached, the flask placed in a heating mantle and the system was purged with argon. The reaction mixture was set on 110 °C and before reaching boiling, Karstedt's catalyst solution ( $10^{-5}$  eq Pt/mol SiH) was added, which resulted in quick increase of temperature and the system starting to reflux. The reaction mixture was kept at the boiling temperature and samples were taken for FT-IR control until full Si-H group consumption was observed. Then, the solvent was evaporated under vacuum to dryness to obtain an analytically pure sample. The products appeared as low-viscosity oils.

### 2.3. Procedure for Preparation of *i*Bu<sub>7</sub>SSQ-OEt

The synthesis was conducted under argon atmosphere in a round-bottom flask equipped with a condenser, a gas bubbler, and a magnetic stirrer. A 500 mL three-neck, round-bottom flask was charged with 15 g of chlorohepta(isobutyl)octasilsesquioxane. A thermometer and condenser equipped with an argon inlet and oil bubbler were attached and the system was purged with argon. After that, the flask was further charged with 250 mL of dry THF and 4.9 mL of NEt<sub>3</sub> (2 eq in correspondence to Si-Cl group), the flask was placed in a heating mantle, and 50 mL of dry EtOH was slowly added. The mixture was heated to 50 °C and stirred for 3 h. Then, the reaction was transferred to a rotary evaporator, the solvent mixture removed almost to dryness, 250 mL of hexane was added to the remaining solid, and the suspension was sonicated for 30 min. The obtained mixture, comprised of the main product solution and triethylammonium hydrochloride suspension, was filtered through a sintered glass funnel to eliminate the ammonium hydrochloride solid, the flask being washed with additional 150 mL of hexane, and the obtained clear hexane solution was evaporated to dryness to obtain analytically pure sample. The product appeared as a white solid.

#### 2.4. Procedure for Treatment of TiO<sub>2</sub> with Organosilicon Compounds

In a typical procedure, a 2.5 L milling jar was charged with 750 g of 50% TiO<sub>2</sub> water slurry, 100 mL of demineralized water (to reduce the mixture viscosity), 20 ceramic milling balls of 20 mm diameter, and either 1.875 g or 5.625 g (corresponding to either 0.5% or 1.5% *w/w* of dry TiO<sub>2</sub>) of a chosen organosilicon coupling agent (see Tables 1 and 2 and Figure 2). The milling jar was closed and placed on the ball mill, and rotated at 30 rpm for 20 h. After that, the slurry was transferred to a container, dried at 105 °C to constant weight and milled again in a ball mill for 20 h. The obtained modified TiO<sub>2</sub> was then sampled for water contact angle measurements and used for preparation of TiO<sub>2</sub>/EP composites. Tests for treatment of TiO<sub>2</sub> with 3% and 5% loadings of organosilicon coupling agents were also performed, but the resulting materials were waxy and/or sticky and difficult to handle, which was a sign of the coupling agents being used in excess. Therefore, only the samples treated with 0.5% and 1.5% of coupling agents were used for further studies.

**Table 1.** Silsesquioxane, spherosilicate, and silane coupling agents used in this study.

Name	Abbreviation
Isobutyltrimethoxysilane	<i>i</i> BuTMOS
3-glycidoxypropyltriethoxysilane	GPTES
ethoxyhepta(isobutyl)octasilsesquioxane	<i>i</i> Bu <sub>7</sub> SSQ-OEt
hexa(3-glycidoxypropyl)di(trimethoxysilylethyl)octaspherosilicate	SS-6GP-2TMOS
penta(3-glycidoxypropyl)tri(trimethoxysilylethyl)octaspherosilicate	SS-5GP-3TMOS

**Table 2.** The TiO<sub>2</sub>/epoxy resin composites prepared in this study.

Sample Name	Organosilicon Coupling Agent Type	Organosilicon Coupling Agent Amount [%] <sup>1</sup>	TiO <sub>2</sub> Amount [%]	Mixing Method	Sample Code
1	none	-	1	Mechanical stirrer	1Ti(s)
2	none	-	1	Mixing pump	1Ti(p)
3	none	-	2	Mixing pump	2Ti(p)
4	<i>i</i> BuTMOS	0.5	1	Mixing pump	1Ti05 <i>i</i> BuTMOS(p)
5	<i>i</i> BuTMOS	0.5	2	Mixing pump	2Ti05 <i>i</i> BuTMOS(p)
6	<i>i</i> BuTMOS	1.5	1	Mechanical stirrer	1Ti15 <i>i</i> BuTMOS(s)
7	<i>i</i> BuTMOS	1.5	1	Mixing pump	1Ti15 <i>i</i> BuTMOS(p)
8	<i>i</i> BuTMOS	1.5	2	Mixing pump	2Ti15 <i>i</i> BuTMOS(p)
9	GPTES	0.5	1	Mixing pump	1Ti05GPTES(p)
10	GPTES	0.5	2	Mixing pump	2Ti05GPTES(p)
11	GPTES	1.5	1	Mechanical stirrer	1Ti15GPTES(s)
12	GPTES	1.5	1	Mixing pump	1Ti15GPTES(p)
13	GPTES	1.5	2	Mixing pump	2Ti15GPTES (p)
14	<i>i</i> Bu <sub>7</sub> SSQ-OEt	0.5	1	Mixing pump	1Ti05 <i>i</i> Bu <sub>7</sub> SSQ-OEt(p)
15	<i>i</i> Bu <sub>7</sub> SSQ-OEt	0.5	2	Mixing pump	2Ti05 <i>i</i> Bu <sub>7</sub> SSQ-OEt(p)
16	<i>i</i> Bu <sub>7</sub> SSQ-OEt	1.5	1	Mechanical stirrer	1Ti15 <i>i</i> Bu <sub>7</sub> SSQ-OEt(s)
17	<i>i</i> Bu <sub>7</sub> SSQ-OEt	1.5	1	Mixing pump	1Ti15 <i>i</i> Bu <sub>7</sub> SSQ-OEt(p)
18	<i>i</i> Bu <sub>7</sub> SSQ-OEt	1.5	2	Mixing pump	2Ti15 <i>i</i> Bu <sub>7</sub> SSQ-OEt(p)
19	SS-6GP-2TMOS	0.5	1	Mixing pump	1Ti05 SS-6GP-2TMOS (p)
20	SS-6GP-2TMOS	0.5	2	Mixing pump	2Ti05 SS-6GP-2TMOS (p)
21	SS-6GP-2TMOS	1.5	1	Mechanical stirrer	1Ti15 SS-6GP-2TMOS (s)
22	SS-6GP-2TMOS	1.5	1	Mixing pump	1Ti15 SS-6GP-2TMOS (p)
23	SS-6GP-2TMOS	1.5	2	Mixing pump	2Ti15 SS-6GP-2TMOS (p)
24	SS-5GP-3TMOS	0.5	1	Mixing pump	1Ti05 SS-5GP-3TMOS (p)
25	SS-5GP-3TMOS	0.5	2	Mixing pump	2Ti05 SS-5GP-3TMOS (p)
26	SS-5GP-3TMOS	1.5	1	Mixing pump	1Ti15 SS-5GP-3TMOS (p)
27	SS-5GP-3TMOS	1.5	2	Mixing pump	2Ti15 SS-5GP-3TMOS (p)

<sup>1</sup> Silane coupling agent amount is given in correspondence to TiO<sub>2</sub>, as *w/w* % of TiO<sub>2</sub>.

### 2.5. Procedure for Preparation of TiO<sub>2</sub>/EP Composites

In a typical procedure, the mixing pump was charged with around 1 kg of base epoxy resin and the stirring was engaged. After 5 min, TiO<sub>2</sub> sample of a given modification grade (see Table 2) was added in an amount corresponding to either 1 wt% or 2 wt% of the final composition and stirred for further 15 min at 800 rpm. After that, the resin mixture was transferred to a container, chilled to room temperature, and sampled for pigment stability tests. Next, the resin mixture was mixed with 12 wt% of the curing agent (Z-1) using a mechanical stirrer, degassed for 5 min in a vacuum chamber, and cast into plates of 4 mm thickness. After 16 h, the plates were removed from the moulds and set for seven days for further curing (see Supplementary Information, Figure S2). After that time, the plates were cut into standardized test specimens for mechanical analysis (dumbbells and bars) with the aid of a CNC milling plotter. The milled specimens were additionally post-cured for 17 h at 70 °C to ensure the most uniform curing state for all tested samples. Such prepared samples were used for mechanical analyses.

For the samples prepared with the mechanical stirrer (Table 2), the resin was mixed with TiO<sub>2</sub> for the same amount of time with the aid of the mechanical stirrer instead of the dissolver, and the rest of the procedure remained unchanged.

The composite sample codes are as follows:

$$x \text{ Ti } y \text{ CODE } (z) \quad (1)$$

where  $x$ —% loading of TiO<sub>2</sub> in the composite;  $y$ —% loading of a given silane coupling agent in correspondence to TiO<sub>2</sub>; CODE—the type of organosilicon coupling agent used (see Table 1, Figure 3);  $z$ —mixing method: ‘s’ for mechanical stirrer, ‘p’ for mixing pump

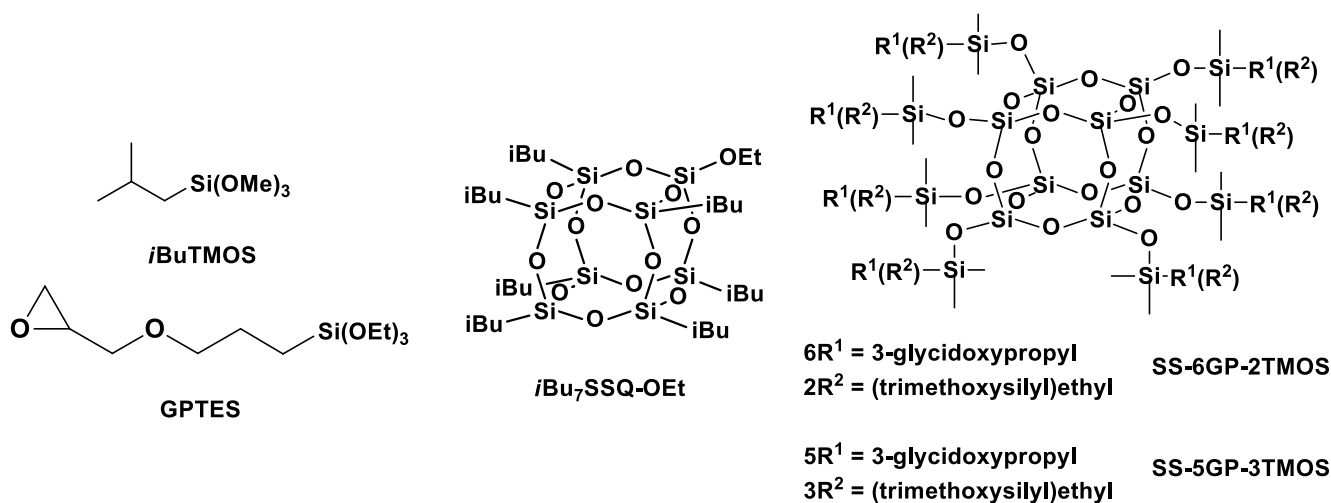


**Figure 3.** Structures of the silane and cage siloxane compounds studied in this work.

## 3. Results and Discussion

### 3.1. Characterization of the Obtained Products

The products were characterized by <sup>1</sup>H, <sup>13</sup>C, <sup>29</sup>Si NMR spectroscopy and MALDI-TOF mass spectrometry to verify the obtained molecular structures (see Supplementary Information). While iBu<sub>7</sub>SSQ-OEt was obtained as a single product, for SS-6GP-2TMOS and SS-5GP-3TMOS, it was observed on MALDI-TOF spectrograms that due to random introduction of the olefin substrates into the spherosilicate cage, a mixture of products was obtained in both cases and nine molecules were formed instead of the one that a given synthesis is designated with. Although the macroscopic stoichiometry of the systems was controlled by using the proper amounts of the olefin reagents, the intramolecular stoichiometry cannot be controlled and the synthesis affords a family of nine congeners, each containing a different internal ratio of organic substituents coming from the parent olefins,

that is, vinyltrimethoxysilane and allyl-glycidyl ether. On the basis of the normalized signal intensity of the congener ions (in a form of sodium ion adducts) recorded by MS, normal distributions similar to Gaussian model were obtained, with the maximum visible near the intended system stoichiometry (Figure 4). Also, the peaks on the left side of the maximum are higher than those on the right for both systems, which can be explained on the basis of different ionization efficiency of glycidyl and alkoxyethyl groups, the glycidyl groups showing higher ionization efficiency. The effect of chemical structure on the ionization efficiency has been studied and discussed by other groups [34,35]. Therefore, this distribution should not be mistakenly considered as a direct depiction of the actual quantitative composition of the studied systems, and rather a qualitative one. It can be seen that for SS-6GP-2TMOS, the maximum is at the SS-7GP-1TMOS congener, which is likely due to the effect discussed above.

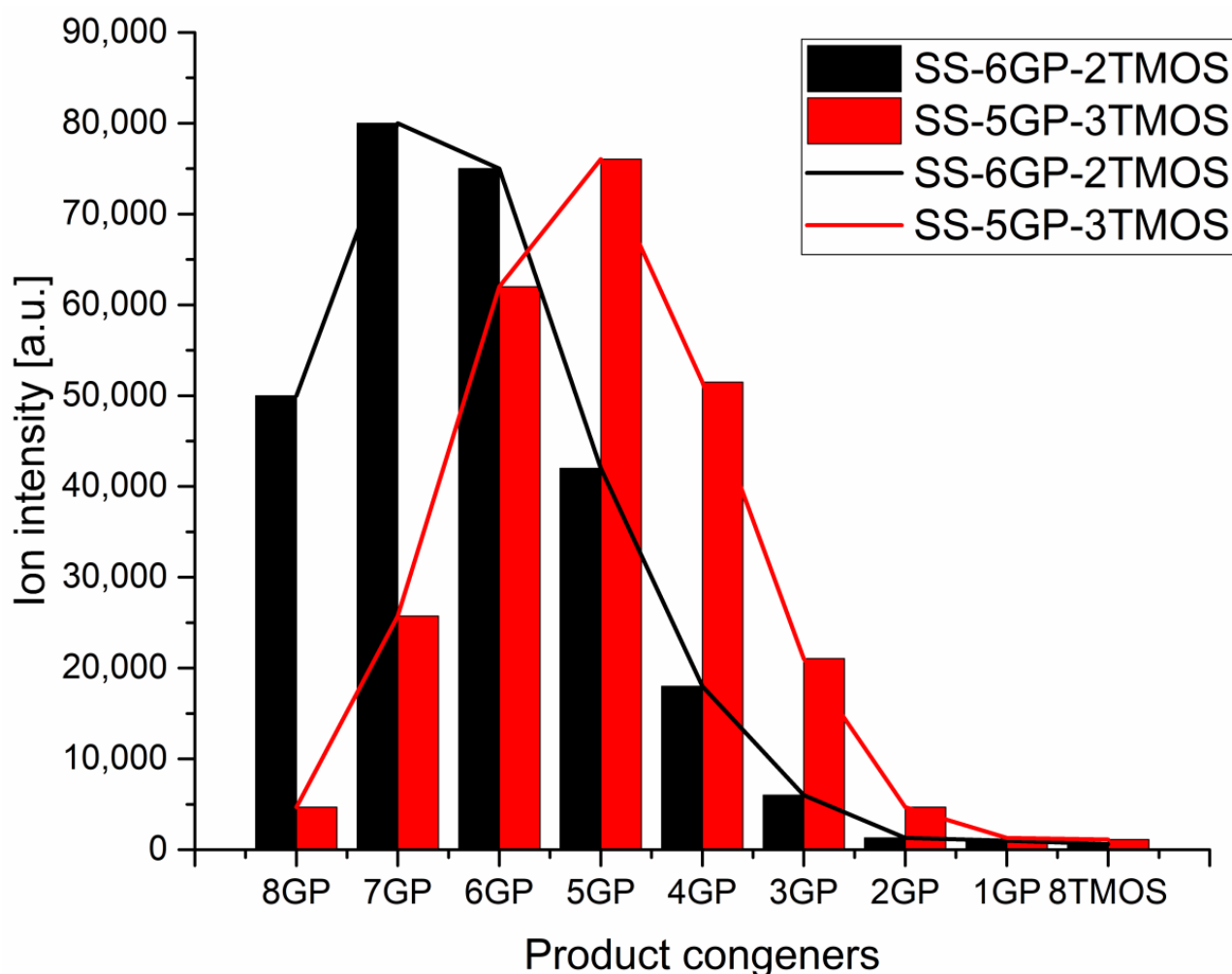


**Figure 4.** Distributions of congener products for SS-6GP-2TMOS and SS-5GP-3TMOS syntheses presented as MS signal intensity.

### 3.2. Surface Properties of the Obtained Modified TiO<sub>2</sub> Pigments

Modified TiO<sub>2</sub> pigments were analysed for their surface properties by measuring their water contact angle values (Table 3). Water contact angle is a non-direct measure of surface polarity of materials, as water is repelled by hydrophobic (non-polar) materials, thus resulting in formation of droplets with high contact angle on the surface of the measured samples. TiO<sub>2</sub>, as an inorganic nanomaterial, shows a strongly polar surface character, which is a reason for the particles thereof to agglomerate in polymer matrices, as they are usually characterized by substantially lower polarity. Introduction of organic (or

organosilicon) groups onto the surface of TiO<sub>2</sub> nanoparticles allows for controlling of their surface character, that is chemistry and polarity. It then translates into better filler-matrix interaction, without which a filler (in this case the pigment) tends to agglomerate [36].

**Table 3.** Water contact angles of TiO<sub>2</sub> modified with the studied silane coupling agents.

Silane Coupling Agent Type	Silane Coupling Agent Amount [%] <sup>1</sup>	Water Contact Angle [°]
None	-	0
<i>i</i> BuTMOS	0.5	0
<i>i</i> BuTMOS	1.5	Superhydrophobic <sup>2</sup>
GPTES	0.5	0
GPTES	1.5	0
<i>i</i> Bu <sub>7</sub> SSQ-OEt	0.5	0
<i>i</i> Bu <sub>7</sub> SSQ-OEt	1.5	Superhydrophobic <sup>2</sup>
SS-6GP-2TMOS	0.5	0
SS-6GP-2TMOS	1.5	0
SS-5GP-3TMOS	0.5	0
SS-5GP-3TMOS	1.5	0

<sup>1</sup> Silane coupling agent amount is given in correspondence to TiO<sub>2</sub>, as *w/w* % of TiO<sub>2</sub>; <sup>2</sup> roll-off observed at each attempt at measuring the contact angle.

The samples treated with any of the glycidyl ether-derived compounds (GPTES, SS-6GP-2TMOS, SS-5GP-3TMOS) showed retainment of their hydrophilic character independently of the amount of the silane agent used, the water droplets being quickly absorbed by the material. It might be either due to polar character of glycidyl group itself, or its partial hydrolysis to even more hydrophilic diol group on the surface of TiO<sub>2</sub>. Kochkar et al. reported that oxirane moiety hydrolyzed to diol one partially when studying epoxidation of cyclohexene on a TiO<sub>2</sub>-SiO<sub>2</sub>-mixed catalyst [37]. This hypothesis is supported by FT-IR spectra of the glycidyl-derived compounds used and the TiO<sub>2</sub> samples modified with those. The IR spectra allow to observe the effect of capping TiO<sub>2</sub> hydroxyl groups, as the –OH stretching band is smaller for modified pigments than for the neat titanium white (Figure 5E, the reduction of absorption intensity marked with shaded area) as well as Ti-O-Si moiety vibrations being visible as a small bulge at ~910 cm<sup>-1</sup> (Figure 5F), which is in agreement with the literature reports [38,39]. Additionally, C-H vibrations are visible, coming from organosilicon additives grafted on the pigment particles surface (Figure 5A,C, green lines). However, while the absorption bands at 1450–1490 cm<sup>-1</sup>, characteristic for C-C oxirane ring vibrations are visible for both the organosilicon compounds and for the obtained pigments (Figure 5B,D, red lines), confirming the successful functionalization thereof, the FT-IR spectra of the latter also show additional absorption bands matching the vibration of the diol C-OH bonds (Figure 5D, blue lines, the oxirane ring opening presented on Figure 8). It is the most clear for the TiO<sub>2</sub>-1.5%GPTES sample, with an absorption band with the maximum at ~1380 cm<sup>-1</sup>, however the remaining modified TiO<sub>2</sub> samples also show similar absorption at ~1385 cm<sup>-1</sup>.

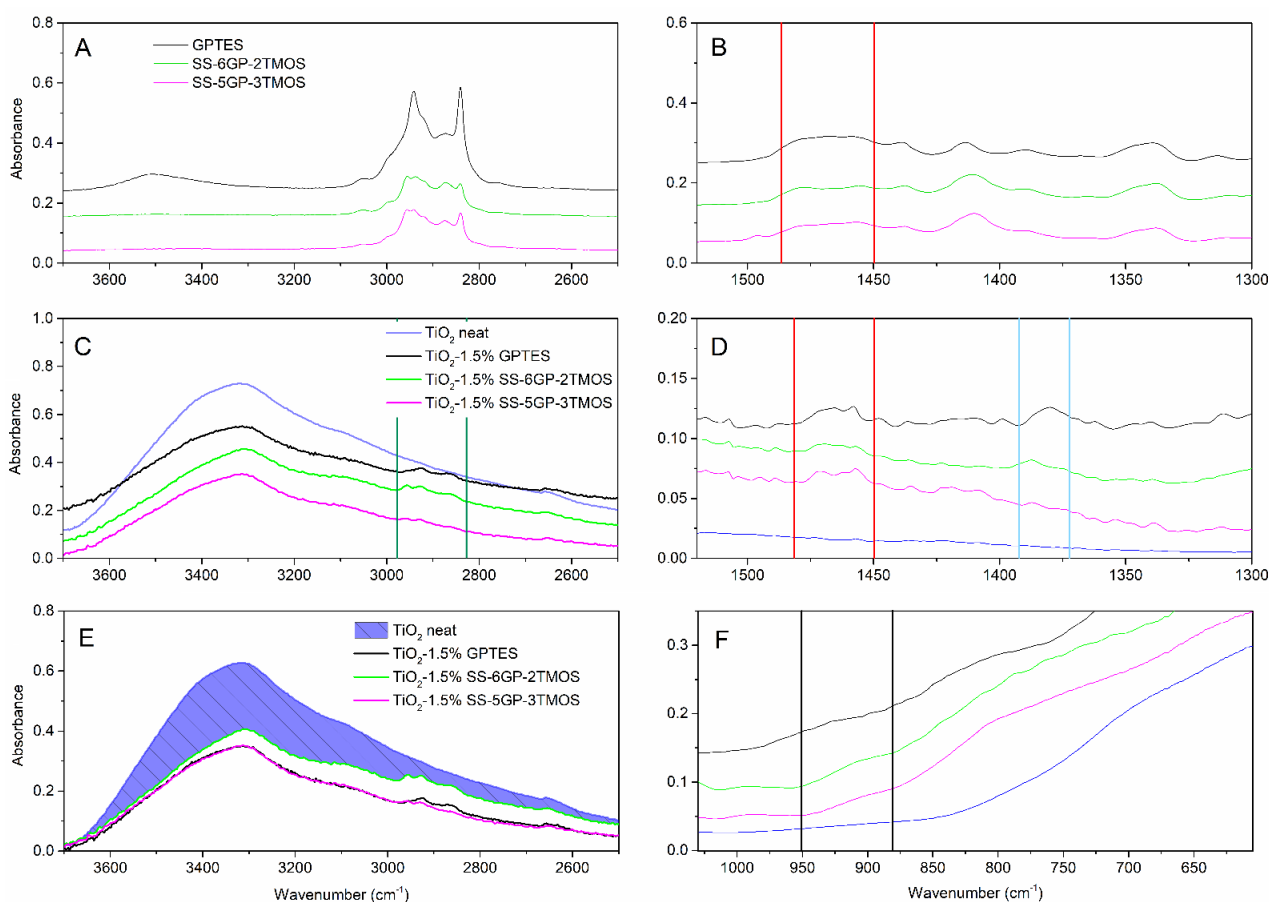


**Figure 5.** FT-IR of glycidyl-derived silane coupling agents (A,B), pristine  $\text{TiO}_2$  and  $\text{TiO}_2$  modified thereof (C–F). Red lines represent the region of oxirane ring vibrations, the blue lines—the diol vibrations, green ones—C-H vibrations, black ones—Ti-O-Si vibrations.

The last effect considered is the gelation of the silane agent, thus reducing the coating effect of the silane agent. SS-6GP-2TMOS was observed on SEM images to form microdroplets accompanying  $\text{TiO}_2$  particles in the final composite (Figure 6A,B visualizing the microdroplets on  $\text{TiO}_2$ , Figure 6D confirming the silicon-rich area on the  $\text{TiO}_2$  microaggregate). On the other hand, butylated agents (both *i*BuTMOS and *i*Bu<sub>7</sub>SSQ-OEt) showed strong hydrophobizing action, as the obtained materials were superhydrophobic. The droplets formed were completely repulsed by  $\text{TiO}_2$ , making it impossible to lay a droplet for the measurement, and when dropped from air, they would immediately roll off even at the angle of  $\sim 0^\circ$  (Figure 7, particles of  $\text{TiO}_2$  visible on the bottom surface of the water droplets after attempts of placing the droplets on the samples' surface).

Based on the FT-IR spectra and water contact angle measurements, proposed mechanisms of  $\text{TiO}_2$  surface functionalization with the studied organosilicon coupling agents is presented on Figure 8.

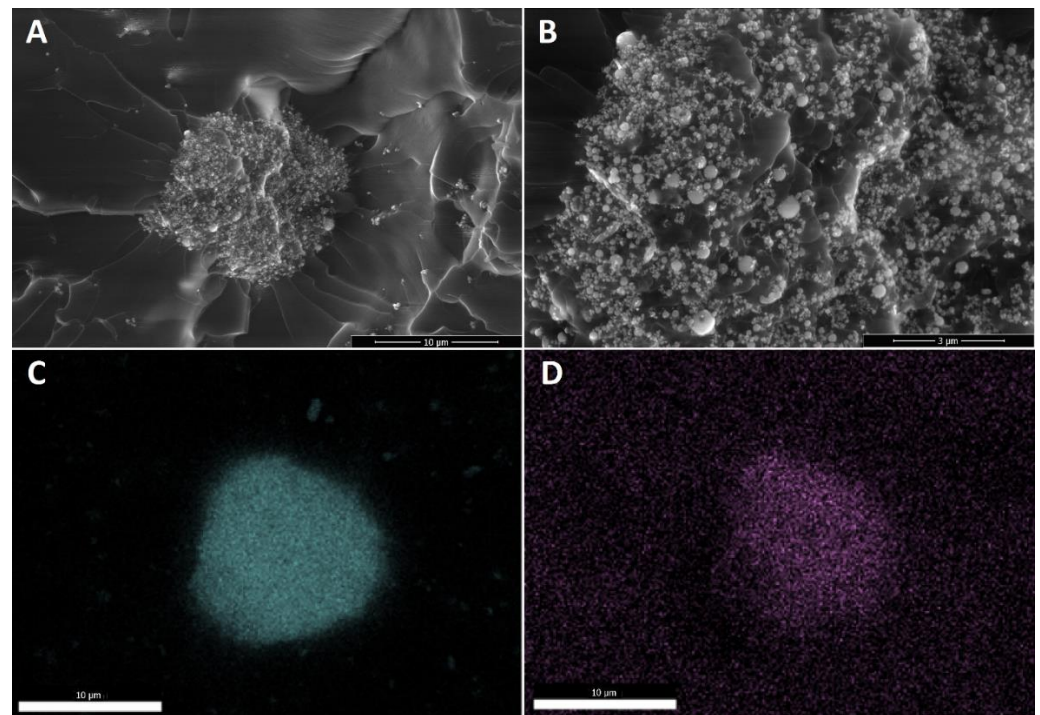


**Figure 6.** Microdroplets of condensed SS-6GP-2TMOS together with  $\text{TiO}_2$  particles visible for 1Ti15SS-6GP-2TMOS. (A)—10,000 $\times$  magnification; (B)—30,000 $\times$  magnification; (C)—titanium (Ti) EDS; (D)—silicon (Si) EDS.

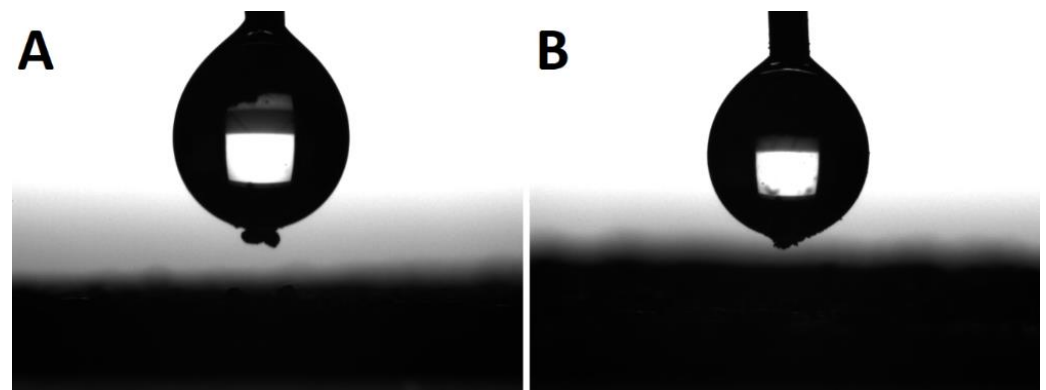


**Figure 7.** Water droplets during sessile drop analysis. Particles of modified  $\text{TiO}_2$  visible on the bottom of each droplet after an attempt at placing the droplet on the pigment surface. (A)— $\text{TiO}_2$ -1.5% *i*BuTMOS; (B)— $\text{TiO}_2$ -1.5% *i*Bu<sub>7</sub>SSQ-OEt.

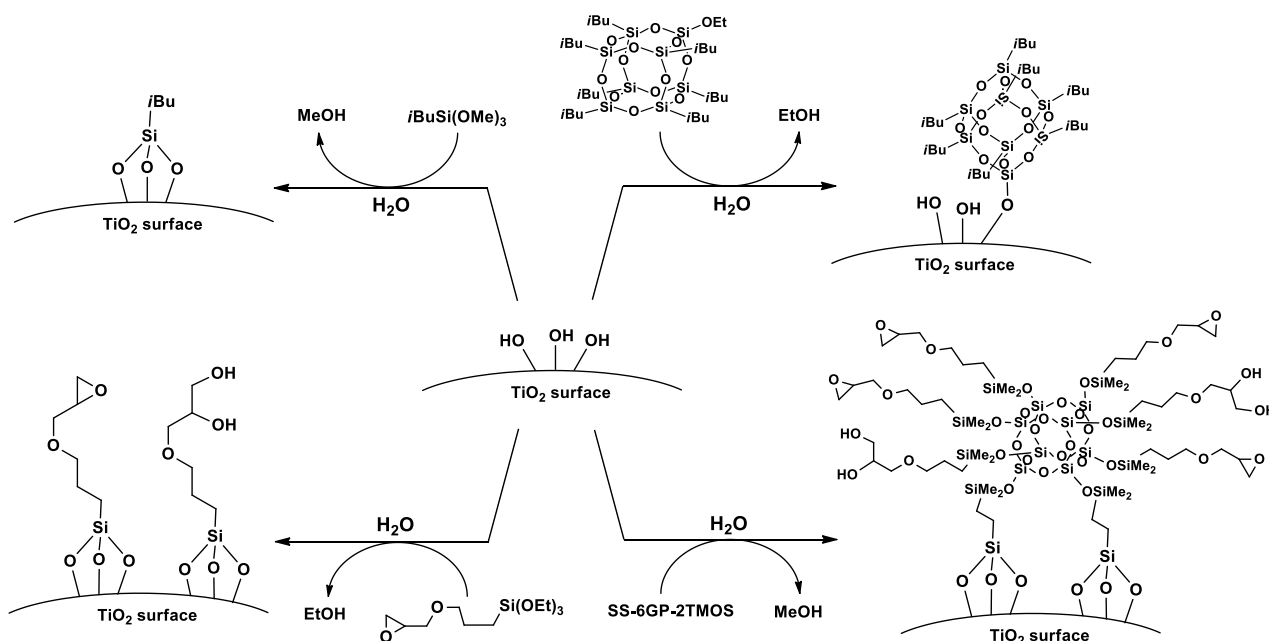


**Figure 8.** A proposed mechanism of  $\text{TiO}_2$  surface silanization with  $i\text{Bu}_7\text{SSQ-OEt}$ ,  $\text{SS-6GP-2TMOS}$  and silane coupling agents.

### 3.3. Microscopic Analysis and the Effect of Processing Methodology on $\text{TiO}_2$ Dispersion

SEM imaging was used to assess the dispersion of  $\text{TiO}_2$  particles in the epoxy matrix (see Supplementary Information Section 4: SEM images of the  $\text{TiO}_2/\text{EP}$  composites). It was observed that the sample prepared with untreated  $\text{TiO}_2$  by mechanical stirring showed the largest agglomeration effect, as not only the particles of  $\text{TiO}_2$  formed multi-micron aggregates of size up to  $50\ \mu\text{m}$ , but also these aggregates were surrounded by barely no well-dispersed microparticles. On the other hand, both high-torque pump stirring and application of organosilicon coupling agents improved the dispersion of the pigment. It is visible on the SEM images of samples containing pristine  $\text{TiO}_2$  that after pump mixing, the primary aggregates observed are of size up to approx.  $20\ \mu\text{m}$ , and that they are accompanied by a fraction of particles of  $<2\ \mu\text{m}$ . Also, for all the sample series, the increase in  $\text{TiO}_2$  loading from 1% to 2% resulted in a higher number of aggregates visible on the SEM images. At 0.5%,  $i\text{BuTMOS}$  was a highly effective dispersing agent both under mechanical stirring and pump stirring conditions, the latter resulting in almost complete elimination of  $\text{TiO}_2$  aggregates above  $2\ \mu\text{m}$ , when the pigment was at the 1% loading. At 1.5%,  $i\text{BuTMOS}$  and 1%  $\text{TiO}_2$  loading, all the pigment was dispersed below  $1\ \mu\text{m}$  after pump mixing, which proved the successful homogenization of the system components. In comparison,  $\text{GPTES}$  was slightly less effective in terms of the size of the aggregates observed, which was especially visible under mechanical stirring.  $i\text{Bu}_7\text{SSQ-OEt}$  was highly effective at dispersing  $\text{TiO}_2$  even when the pigment was at the 2% loading. When compared to simple silane coupling agents (trialkoxysilanes),  $i\text{Bu}_7\text{SSQ-OEt}$  does not have the ability to form gel products (polysilsesquioxanes), which, depending on the silane: filler ratio and processing conditions, may cause secondary aggregation of  $\text{TiO}_2$  by binding the particles together with polysilsesquioxane gel.  $\text{SS-6GP-2TMOS}$  effectively dispersed the pigment at 0.5% additive loading for both 1% and 2% of  $\text{TiO}_2$  used, while at the higher loading of silane agent, aggregation was observed due to the agent gelation. The gelling effect was more visible for  $\text{SS-5GP-3TMOS}$ , however the additive still allowed for elimination of larger ( $>10\ \mu\text{m}$ ) primary agglomerates. In addition, the dispersing effect of a selected modifier,  $i\text{Bu}_7\text{SSQ-OEt}$ , was visualized with aid of digital optical microscopy (Figure 9), where diluted samples containing 0.0625%  $\text{TiO}_2$  (see Section 3.4. Pigment Stability and Hiding Power Studies) were observed in light transmission mode. For the samples containing modified  $\text{TiO}_2$ , a significant drop in abundance of larger pigment agglomerates was observed, and in their place,

even graininess effect was visible, which corresponded to the presence of finely dispersed pigment particles, as confirmed with detailed SEM imaging discussed above (for SEM images, see Supplementary Information Section 4: SEM images of the TiO<sub>2</sub>/EP composites).

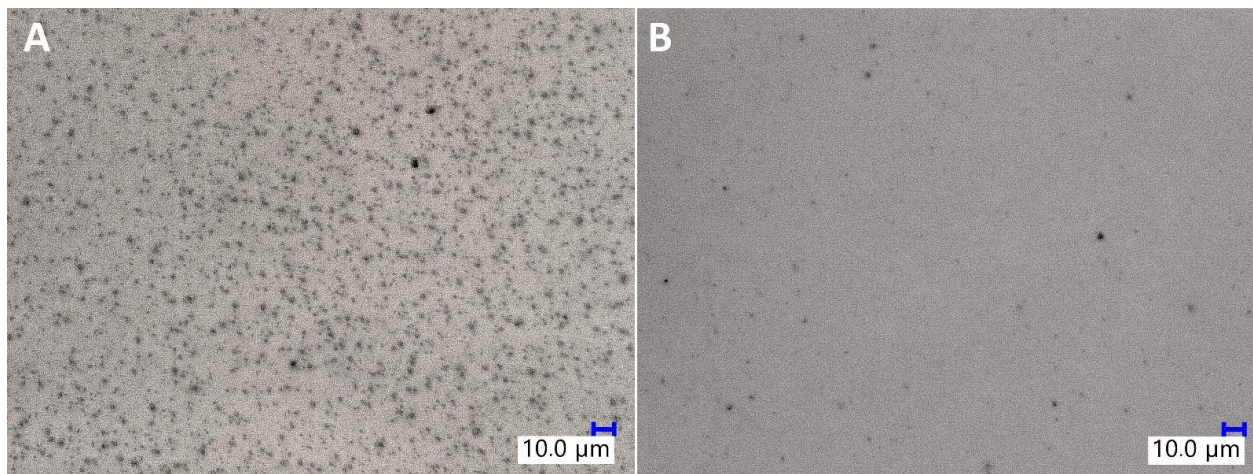


**Figure 9.** Digital optical microscopic images of neat TiO<sub>2</sub>/EP (A) and 1.5% *i*Bu<sub>7</sub>SSQ-OEt TiO<sub>2</sub>/EP (B).

### 3.4. Pigment Stability and Hiding Power Studies

The stability of modified and pristine TiO<sub>2</sub>/liquid epoxy resin suspensions was assessed by pouring samples of the suspensions in screw-capped centrifuge vials and leaving them on standing. Then, they were checked every couple of days for any signs of phase separation, including pigment precipitation on the vial walls or bottom, resin cloudiness, or discoloration near the surface. The samples prepared by mechanical stirring all underwent heavy phase separation within two weeks from preparation, as the larger agglomerates of TiO<sub>2</sub> were characterized by poor stability in the suspension. It correlates with the SEM images (Supplementary Information), as these larger agglomerates were captured. On the other hand, the samples prepared by high shear pump mixing showed much higher suspension stability, the improved dispersing method increasing the stability time by over an order of magnitude for some of the studied systems (Figure 10). The main conclusion obvious from the results obtained is that, independently of the discussed TiO<sub>2</sub> system used, increasing pigment loading from 1% to 2% resulted in more or less severe reduction in the suspension stability. It can be understood as higher concentration of TiO<sub>2</sub> particles in the epoxy suspension causing their faster aggregation over storage time; however, the SEM images of TiO<sub>2</sub>/EP composites made from freshly prepared suspensions also revealed increased agglomeration in the composites containing 2% of TiO<sub>2</sub>. These results suggest that for the TiO<sub>2</sub> pigments of limited stability, formation of primary agglomerates (<10 μm) is a fast process, after which these agglomerates grow at the rate depending on the pigment concentration in the suspension and the surface physicochemistry of the particles, up to the point of spontaneous sedimentation. This idea is further supported by the results of hiding power study (Figure 11). Interestingly, some of the studied coupling agents provided virtually no stabilization to the pigment over prolonged time, that is, SS-6GP-2TMOS at 0.5% loading and SS-5GP-3TMOS at both loadings. It may be due to the protic character of the diol groups generated during surface coupling of TiO<sub>2</sub>, resulting in interparticle attraction, but also less effective particle coating with the coupling agent and the gelling thereof, as discussed earlier (Section 3.2. *Surface Properties of the Obtained Modified TiO<sub>2</sub> Pigments*). GPTES showed behaviour comparable to that of SS-6GP-2TMOS. On the other hand, *i*Bu<sub>7</sub>SSQ-OEt at 0.5% loading provided stabilization superior to all the other coupling agents studied, and at 1.5% loading, slightly higher than that of *i*BuTMOS. It is due to the apolar character of the isobutyl group, which both the SSQ and silane compounds share in common.

The studies of hiding power based on the samples' visible light transmittance revealed the effect of both processing technique and coupling agent choice on the pigmentation efficacy of the resulting epoxy systems. While application of modified  $\text{TiO}_2$  via mechanical stirring resulted in slight improvement of hiding power (approximately two-fold on the average of the studied systems), and the implementation of pump mixing allowed for a more significant improvement (over five-fold for neat  $\text{TiO}_2$  at 1% loading), the most impressive results were obtained when both surface treatment and pump mixing were applied. It proves that chemical modification of the pigment particles results not only in enhanced dispersability thereof in the epoxy during suspension preparation, but also stabilizes these particles in the suspension, hampering their secondary self-aggregation. For neat  $\text{TiO}_2$ , increasing the pigment loading from 1% to 2% resulted in only 17% increase of hiding power, making little change in the overall performance of the composition. On the other hand, for the systems containing  $\text{TiO}_2$  treated with 0.5% of *i*Bu<sub>7</sub>SSQ-OEt it was 59% increase; for 0.5% and 1.5% of SS-6GP-2TMOS, 679% and 300%, respectively; for 0.5% and 1.5% of SS-5GP-3TMOS, 958% and 1490%, respectively. Interestingly, despite showing moderate to poor stability over storage time, the discussed spherosilicate-based modifiers still performed well at enhancing pigmentation efficacy of the  $\text{TiO}_2$  treated thereof. The best performing pigment system was pump-mixed  $\text{TiO}_2$  treated with 1.5% of *i*Bu<sub>7</sub>SSQ-OEt, where at 1%  $\text{TiO}_2$  loading, the relative hiding power was over ten times higher than that of the sample containing pump-mixed neat  $\text{TiO}_2$ ; at 2% loading, the hiding power was nine times higher than that of the neat pigment counterpart.

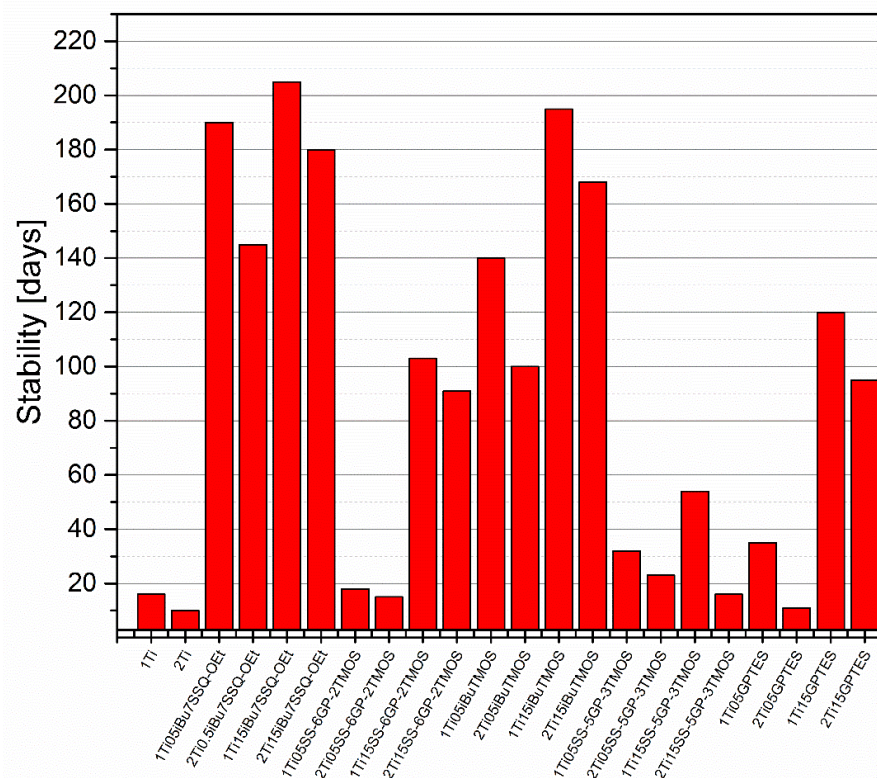


**Figure 10.** Time-dependent stability of  $\text{TiO}_2$  suspensions in liquid epoxy systems prepared by pump mixing.

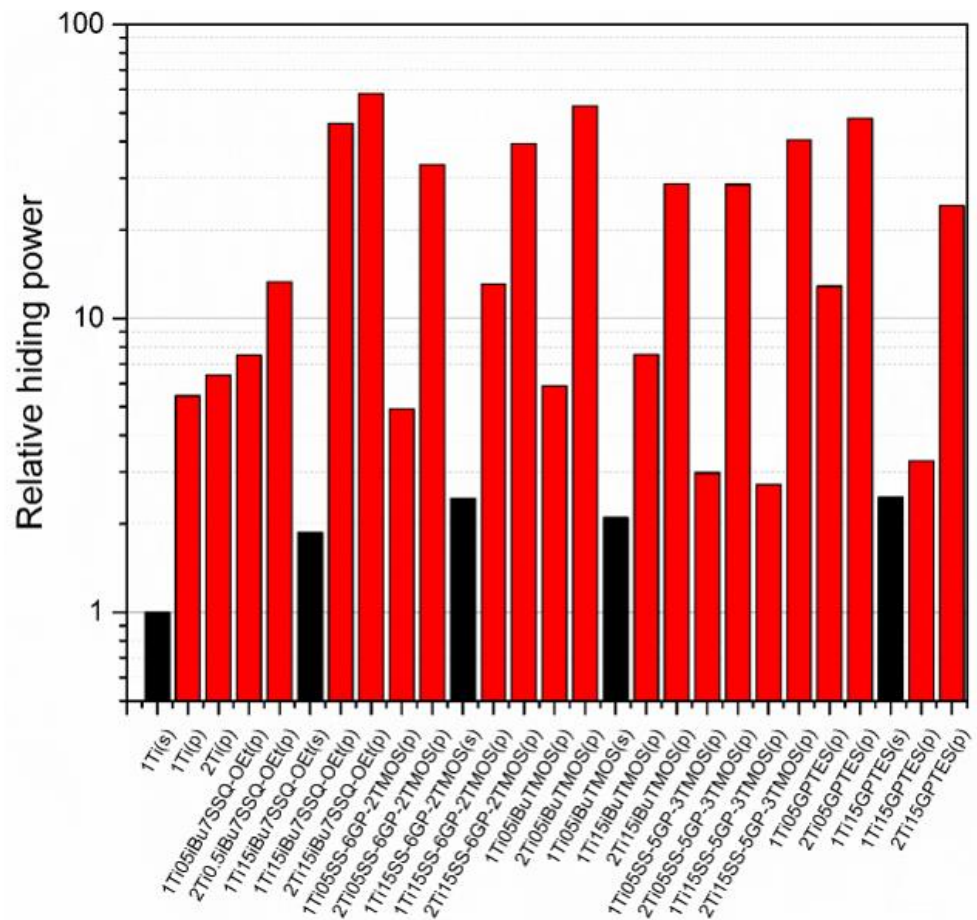


**Figure 11.** Relative hiding power of the pigmented epoxy systems.

To visualise the practical effect of improved  $\text{TiO}_2$  dispersion within the epoxy base, an additional experiment was performed where a sample of a chosen epoxy containing 1% of modified  $\text{TiO}_2$  and a series of dilutions was prepared with neat epoxy to obtain samples of 0.5%, 0.25%, 0.125%, and 0.0625% of  $\text{TiO}_2$  (Figure 12, the last concentration omitted due to poor pigmentation). After that, pigmentation was evaluated comparatively between the series of samples by assessing their visual opaqueness on a colourful background. While the samples containing neat  $\text{TiO}_2$  were already visibly transparent at 0.5% loading, the samples containing 1.5% *i*Bu<sub>7</sub>SSQ-OEt-modified  $\text{TiO}_2$  provided satisfactory pigmentation up to the 0.25% dilution.

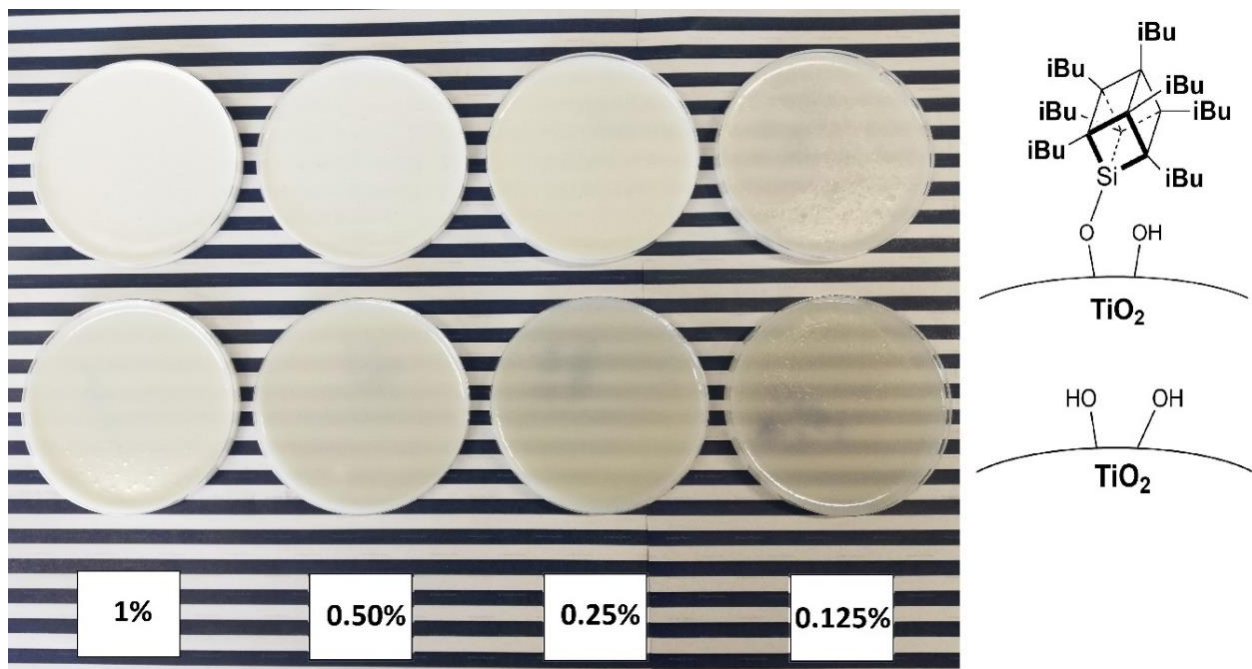


**Figure 12.** Serial dilution samples of mixing pump-prepared 1.5% *i*Bu<sub>7</sub>SSQ-OEt TiO<sub>2</sub>/EP (top) and neat TiO<sub>2</sub>/EP (bottom).

### 3.5. Mechanical Studies

Mechanical analysis revealed subtle differences between the TiO<sub>2</sub>/epoxy systems studied, even despite low loading of TiO<sub>2</sub> in the composites (Figures 13–16). For Young's modulus, it was observed that the systems present stiffness comparable to the neat epoxy within the limits of the standard deviation (Figure 14). Also, for the samples containing either 1% or 2% of the same type of prepared TiO<sub>2</sub> (either pristine or modified), there was a tendency towards Young's modulus increase along with the pigment concentration for well-dispersed systems (e.g., 0.5% *i*Bu<sub>7</sub>SSQ-OEt/TiO<sub>2</sub>, 0.5% *i*BuTMOS/TiO<sub>2</sub>), while for the agglomerating pigments, the value would drop (e.g., pristine TiO<sub>2</sub>, 0.5% GPTES/TiO<sub>2</sub>). Due to low loadings of the pigmenting filler used, retention of tensile properties (tensile strength and elongation at break, that is) should rather be considered instead of their improvement, as the loading of the filler is too small to provide enough reinforcement and the mechanical failure may propagate throughout the bulk polymer. For tensile strength, mechanical stirrer-prepared composites were the weakest from each series, as the agglomerated particles provided spots of structural imperfection, causing material failure. Some of the highest values of tensile strength and elongation at break were recorded for systems loaded with TiO<sub>2</sub> modified with 1.5% of SS-6GP-2TMOS and 0.5% of SS-5GP-3TMOS due to high dispersion and well-developed particle-polymer interphase. Also, *i*Bu<sub>7</sub>SSQ-OEt/TiO<sub>2</sub>, performed slightly better than its silane counterpart system, *i*BuTMOS/TiO<sub>2</sub>, suggesting that silsesquioxane- and spherosilicate-based coupling agents provide better surface treatment agents, likely due to less gelation side reactions.

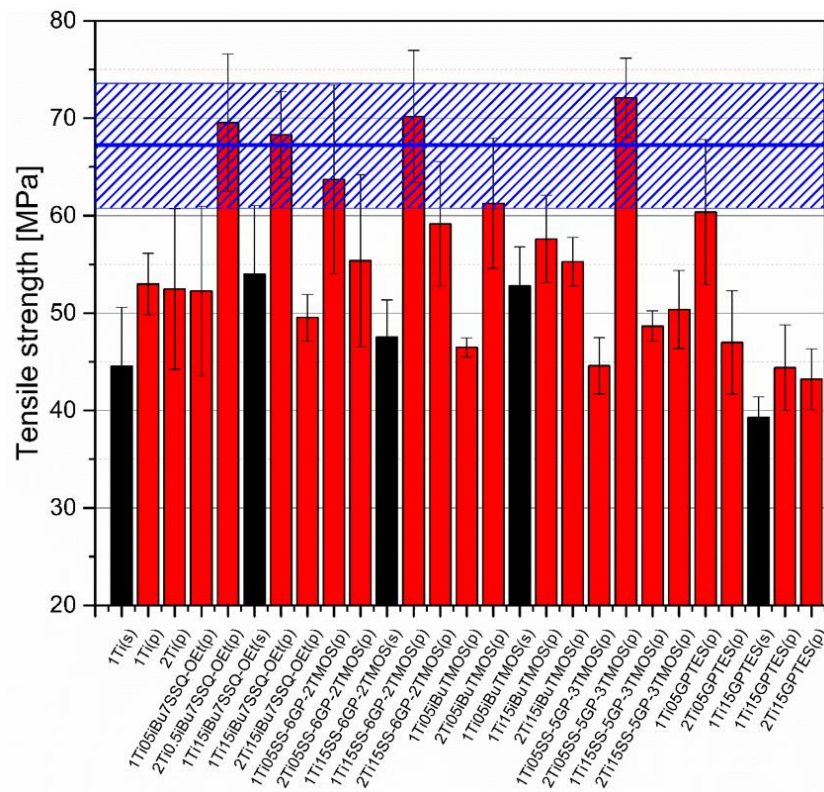


Figure 13. Tensile strength of neat and modified TiO<sub>2</sub>/EP composites.

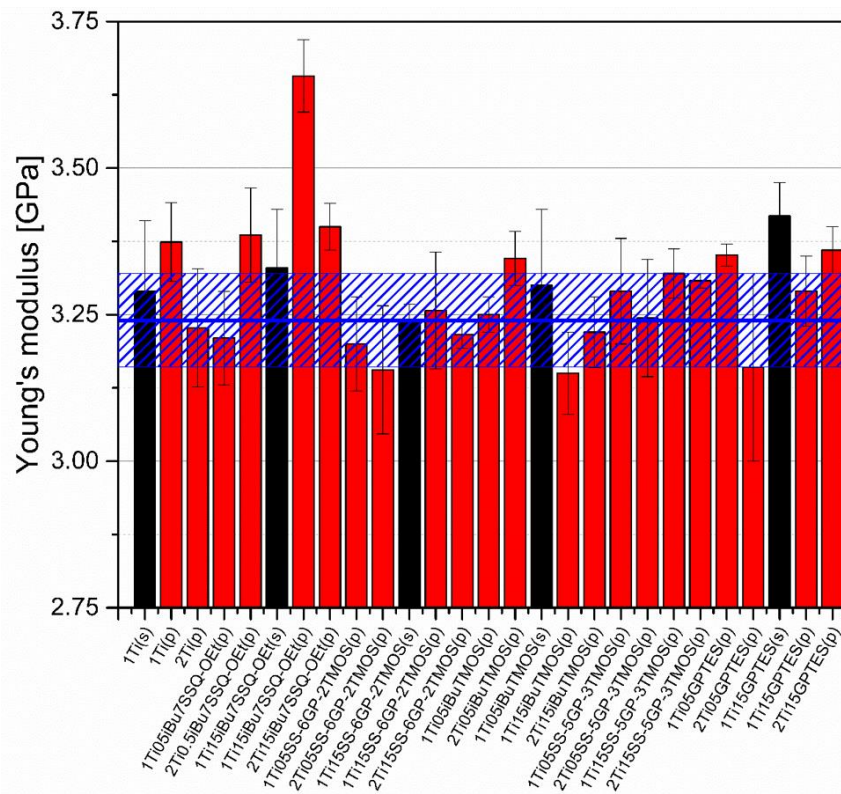


Figure 14. Young's modulus of neat and modified TiO<sub>2</sub>/EP composites.

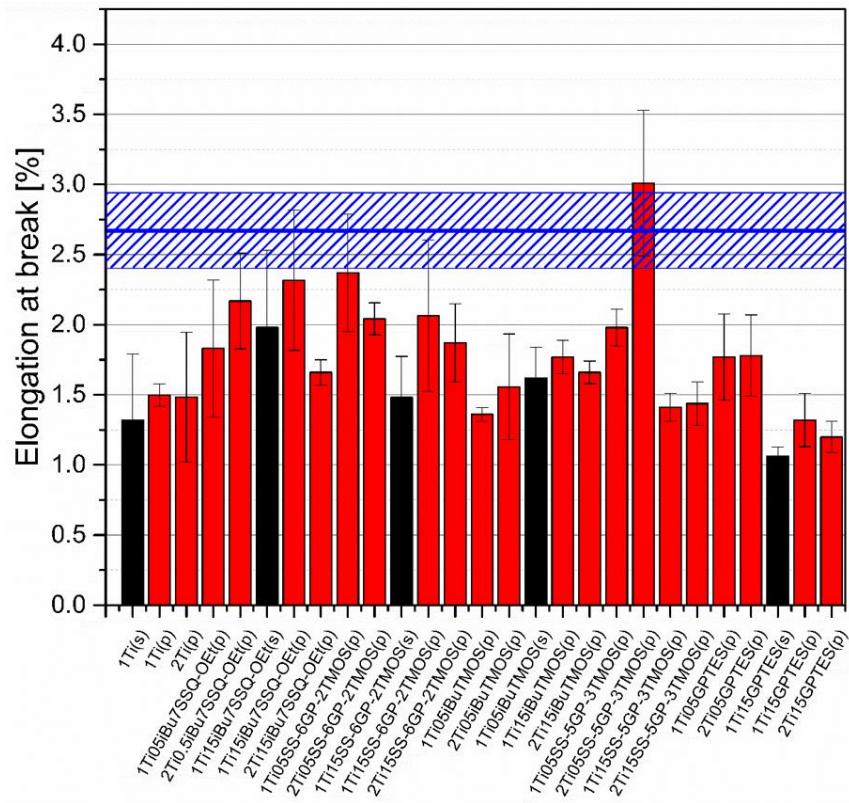


Figure 15. Elongation at break of neat and modified TiO<sub>2</sub>/EP composites.

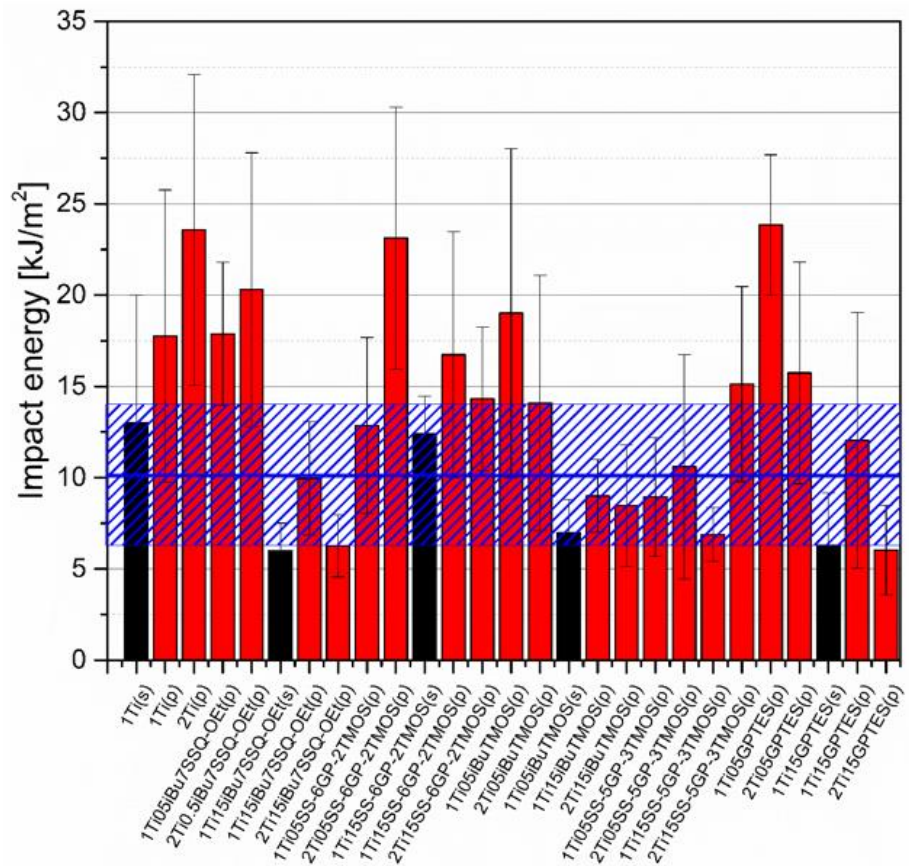


Figure 16. Impact energy of neat and modified TiO<sub>2</sub>/EP composites.

Impact resistance tests revealed that some of the prepared systems were characterized by up to over 100% increase in durability described by the mean impact energy (Figure 16). Among those, samples containing pristine TiO<sub>2</sub> showed satisfactory performance and that the systems of the highest dispersion of the pigment are not the ones of the highest impact resistance. This proves that the agglomerates and particles of moderate size may work as crack propagation interrupters. Findings supporting such statement were reported earlier when studying diatomite-filled epoxy composites [40]. Triethylenetetramine-cured epoxy resins under low temperatures and high strain rates tend to undergo continuous crack propagation and such heterogeneous regions introduced in the polymer bulk may help to discontinue this propagation [41].

### 3.6. Thermal Studies

Although the studied materials share the same polymer matrix and the base pig-menting filler, the preparation methodology applied and the coupling agent used cause subtle structural and interfacial differences that can be elucidated with DSC (Figure 17, top). Epoxy systems of similar polymer matrix were studied earlier [40,42]. It can be seen that for the second heating cycle, the  $T_g$  of most of the samples appears at ~120 °C, being close to that of the neat epoxy (Figure 17, bottom). However, for the mechanical stirrer-prepared compositions, the  $T_g$  was observed to be slightly lowered for all examples, both compared to the mixing pump-prepared ones and the neat epoxy. It has been a subject of discussion that fillers presenting weak interaction with the polymer tend to reduce  $T_g$  by creating an interface where due to poor filler surface wetting action, a fraction of polymer is formed, characterized by more freedom than that of the bulk polymer [43–45]. By this thesis, it can be explained that the poorly dispersed TiO<sub>2</sub> particles create such interface due to their reduced surface/volume ratio. Another observation was made on the change of  $T_g$  over time. Two measurements were taken 21 days apart, after seven and 30 days of resin casting. By the time of the second measurement,  $T_g$  would increase by average of two degrees Celsius for most samples, as additional diffusion between the epoxy and TiO<sub>2</sub> occurred over time. The effect was less prominent for the samples containing GPTES-treated TiO<sub>2</sub>, suggesting stronger and less elastic grafting of the epoxy chains on the modified particles in the first place. Similar behaviour of nanocomposites containing fillers with reactive group-containing coupling agents was described by Ash, Schadler et al. [45]. Additionally, the glass transition of epoxy composites with no thermal treatment was studied (glass transition of residually uncured resin,  $T_{gu}$ , Figure 17, middle). In this case, the phenomenon of low-temperature glass transition is caused mostly by the bulk resin, with polymer domains containing highly flexible chains containing either unreacted oxirane or amine groups. These chains undergo further partial cross-linking upon sample aging, but for more complete curing, samples need to be heated above that  $T_{gu}$  temperature for the unreacted chains to regain mobility and undergo further cross-linking. As was mentioned, this phenomenon is caused by the bulk material and by so, the filler has a very small and unclear effect on the  $T_{gu}$  values. For the studied systems,  $T_{gu}$  was in a 52–54 °C range for all the samples after seven days from casting, and after 30 days the value would increase by average of 6 °C. The highest  $\Delta T_{gu}$  were observed for the samples containing TiO<sub>2</sub> treated with 1.5% of GPTES and spherosilicate agents, and prepared by mixing pump, supporting the abovementioned hypothesis that the well-dispersed, modified nanoparticles undergo grafting of epoxy chains on their surface, which introduces regions of decreased chain mobility within the matrix. The effect was less prominent for the remaining modifiers, suggesting more mobile nanoparticle-matrix interphase caused by the non-covalent interactions.

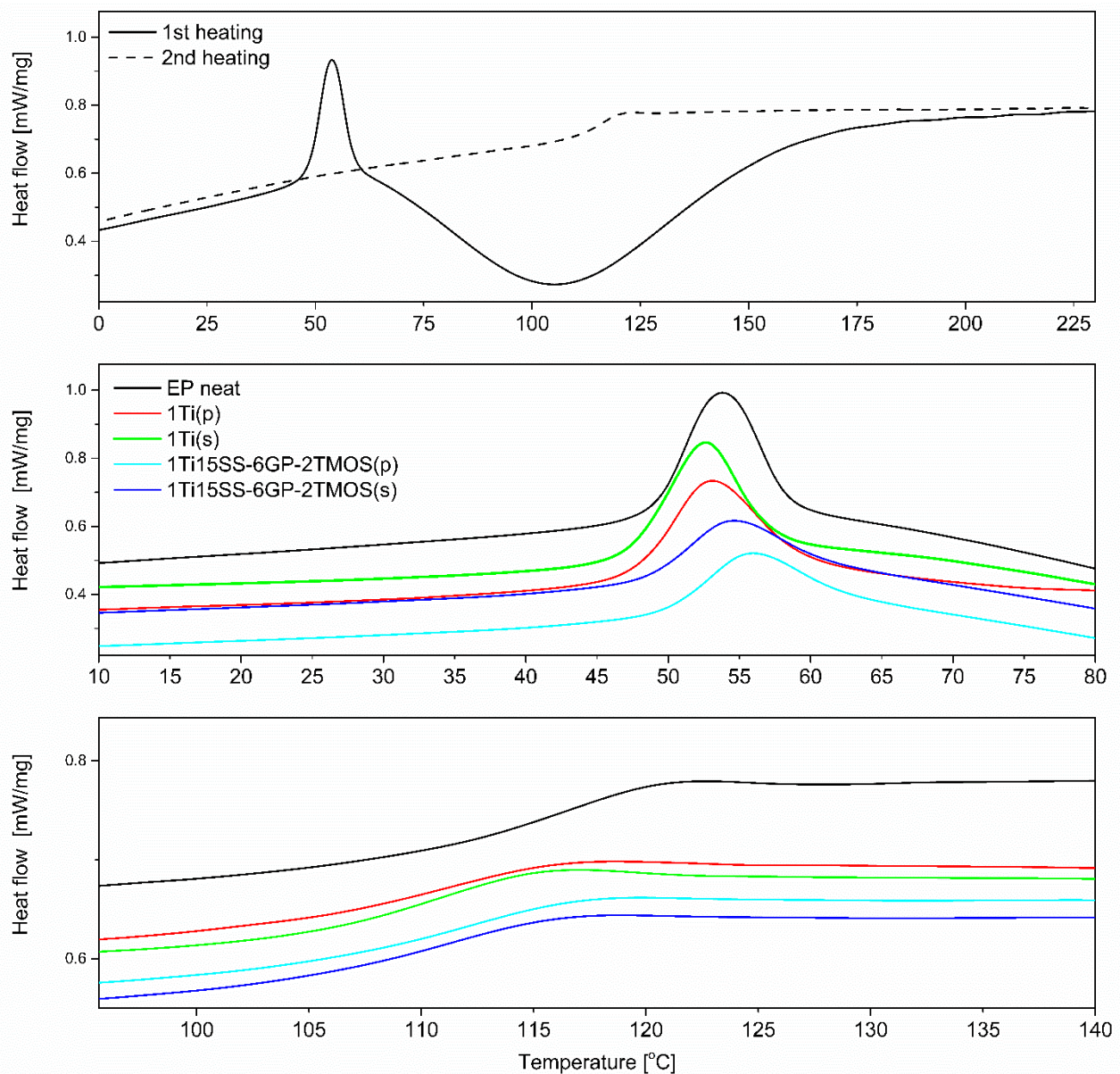


Figure 17. DSC plots of selected epoxy systems; neat EP (top);  $T_{gu}$  region (middle),  $T_g$  region (bottom).

#### 4. Conclusions

The conclusions to be drawn from this study, are:

(1) A novel method for preparation of highly dispersed  $\text{TiO}_2$ /epoxy systems with the aid of a custom high-shear gear pump was presented. The impact of the pigment dispersing method on the properties of epoxy systems has been discussed in detail, including suspension stability and composite hiding power. It was shown that physical means of dispersing the nanoparticles are as much important as the chemical ones for their surface treatment, and together, a synergistic effect is obtained.

(2) An effective and green method for  $\text{TiO}_2$  surface treatment in aqueous media was described. Herein the method may be introduced into the production line of  $\text{TiO}_2$  pigments for coating/paint industry, if professional application of such systems was to be considered.

(3) Improved mechanical properties were observed in terms of impact resistance and Young's modulus, when silsesquioxane coupling agent was used, due to good dispersion of the nanoparticles within the epoxy matrix.

(4) High hiding power was obtained with the described methodology including both chemical surface treatment of the  $\text{TiO}_2$  pigment and high-shear dispersing procedure

thereof, proving the synergistic effect of the two. The proposed methodology may serve for preparation of novel, high-performance coating systems. Additionally, improved dispersion and particle stability may allow for reduction of pigment loading for the epoxy base to obtain the satisfactory hiding power.

(5) TiO<sub>2</sub> dispersions of long shelf life were obtained, the selected cage siloxane additives showing superior stabilizing effect over silane coupling agents.

(6) Superhydrophobic effect for TiO<sub>2</sub> surface was obtained for two coupling agents—*t*-BuTMOS and *t*-Bu<sub>7</sub>SSQ-OEt, showing the great possibilities in terms of modification of the surface properties of TiO<sub>2</sub> with the application of silsesquioxane agents.

(7) The chemical reactions occurring during TiO<sub>2</sub> surface modification were proposed and confirmed with FT-IR. The hydrolytic opening of oxirane ring to the corresponding diol has been confirmed, possibly catalysed by TiO<sub>2</sub> itself, which is an important finding concerning surface treatment of similar materials in water-based media.

The obtained findings show that the silsesquioxane- and spherosilicate-based coupling agents are somehow similar to their silane counterparts, but have their advantages over simple silanes. It might encourage tuning of silsesquioxane compounds structure and the process of their application, if their use as surface treatment agents is sought for special applications, e.g., high performance coating systems.

**Supplementary Materials:** The following are available online at <https://www.mdpi.com/article/10.3390/ma15020494/s1>, Figure S1. Internal gear pump setup used for preparation of TiO<sub>2</sub>/epoxy dispersions; Figure S2. A sample of cured TiO<sub>2</sub>/epoxy composite prepared; NMR spectroscopy of the obtained compounds; MALDI-TOF mass spectra of obtained spherosilicate compounds; SEM images of the TiO<sub>2</sub>/EP composites.

**Author Contributions:** Conceptualization, D.B. and R.E.P.; Data curation, D.B., M.F., D.P., M.D. and B.S.; Formal analysis, D.B., M.F., D.P., M.D. and B.S.; Funding acquisition, D.B. and B.M.; Investigation, D.B. and R.E.P.; Methodology, R.E.P.; Project administration, D.B. and R.E.P.; Resources, D.B.; Software, D.B., M.F., D.P. and M.D.; Supervision, R.E.P. and B.M.; Validation, R.E.P.; Visualization, D.B., M.F., D.P., M.D. and B.S.; Writing—original draft, D.B., R.E.P., M.F. and D.P. All authors have read and agreed to the published version of the manuscript.

**Funding:** This research was funded by the National Science Centre, Poland, grant number UMO-2018/29/N/ST5/00868 and UMO/2017/27/B/ST5/00149.

**Institutional Review Board Statement:** Not applicable.

**Informed Consent Statement:** Not applicable.

**Data Availability Statement:** All the data were collected and provided either in the main manuscript file or in the Supplementary Materials File.

**Conflicts of Interest:** The authors declare no conflict of interest.

## References

1. Chanda, M.; Roy, S.K. *Industrial Polymers, Specialty Polymers, and Their Applications*; CRC Press: Boca Raton, FL, USA, 2009.
2. Xanthos, M. *Functional Fillers for Plastics*, 2nd ed.; Wiley-VCH: Weinheim, Germany, 2010.
3. Faulkner, E.B.; Schwartz, R.J. *High Performance Pigments*, 2nd ed.; Wiley-VCH: Weinheim, Germany, 2009.
4. Buxbaum, G.; Pfaff, G. *Industrial Inorganic Pigments*, 3rd ed.; Wiley-VCH: Weinheim, Germany, 2005.
5. Available online: <https://www.icis.com/explore/resources/news/2020/04/17/10497512/europe-tio2-demand-buffed-by-coronavirus-headwinds-loom> (accessed on 8 November 2021).
6. Dong, X.; Zhang, X.; Yu, X.; Jiang, Z.; Liu, X.; Li, C.; Sun, Z.; Zheng, S.; Dionysiou, D.D. A novel rutile TiO<sub>2</sub>/AlPO<sub>4</sub> core-shell pigment with substantially suppressed photoactivity and enhanced dispersion stability. *Powder Technol.* **2020**, *366*, 537–545. [[CrossRef](#)]
7. Xue, B.; Yan, R.; Wang, C.; Zhang, H.; Yue, Y.; Luo, J. Study on the characterization technology of hiding power of powder coating. *J. Phys. Conf. Ser.* **2021**, *1965*, 012046. [[CrossRef](#)]
8. Plueddeman, E.P. *Silane Coupling Agents*, 2nd ed.; Springer Science + Business Media: New York, NY, USA, 1991.
9. Koksziel, J. *Materiały Polimerowe*; Wydawnictwo Politechniki Częstochowskiej: Częstochowa, Poland, 1999.
10. Misasi, J.M.; Jin, Q.; Knauer, K.M.; Morgan, S.E.; Wiggins, J.S. Hybrid POSS-Hyperbranched polymer additives for simultaneous reinforcement and toughness improvements in epoxy networks. *Polymer* **2017**, *117*, 54–63. [[CrossRef](#)]

11. Liu, Y.-L.; Chang, G.-P. Novel approach to preparing epoxy/polyhedral oligometric silsesquioxane hybrid materials possessing high mass fractions of polyhedral oligometric silsesquioxane and good homogeneity. *J. Polym. Sci. Part A Polym. Chem.* **2006**, *44*, 1869–1876. [[CrossRef](#)]
12. Strachota, A.; Whelan, P.; Kříž, J.; Brus, J.; Urbanová, M.; Šlouf, M.; Matějka, L. Formation of nanostructured epoxy networks containing polyhedral oligomeric silsesquioxane (POSS) blocks. *Polymer* **2007**, *48*, 3041–3058. [[CrossRef](#)]
13. Brus, J.; Urbanová, M.; Strachota, A. Epoxy Networks Reinforced with Polyhedral Oligomeric Silsesquioxanes: Structure and Segmental Dynamics as Studied by Solid-State NMR. *Macromolecules* **2008**, *41*, 372–386. [[CrossRef](#)]
14. Suliga, A.; Hamerton, I.; Viquerat, A. Cycloaliphatic epoxy-based hybrid nanocomposites reinforced with POSS or nanosilica for improved environmental stability in low Earth orbit. *Compos. Part B Eng.* **2018**, *138*, 66–76. [[CrossRef](#)]
15. Frechette, M.F.; Anh, T.T.; Heid, T.; Vanga-Bouanga, C.; Ghafarizadeh, S.B.; David, E.; El-Khoury, D.; Castellon, J. Dielectric properties of epoxy composites containing both molecular and nanoparticulate silica. In Proceedings of the 2016 IEEE Conference on Electrical Insulation and Dielectric Phenomena (CEIDP), Toronto, ON, Canada, 16–19 October 2016. [[CrossRef](#)]
16. Longhi, M.; Pistor, V.; Zini, L.P.; Kunst, S.R.; Zattera, A.J. Influence of Functionality of Polyhedral Oligomeric Silsesquioxane (POSS) Dispersed in Epoxy Resin for Application in Hybrid Coating. *Mater. Sci. Forum* **2017**, *899*, 278–282. [[CrossRef](#)]
17. Heid, T.; Frechette, M.; David, E. Dielectric properties of epoxy/POSS composites. In Proceedings of the 2013 Annual Report Conference on Electrical Insulation and Dielectric Phenomena, Shenzhen, China, 20–23 October 2013. [[CrossRef](#)]
18. Huang, X.; Li, Y.; Liu, F.; Jiang, P.; Iizuka, T.; Tatsumi, K.; Tanaka, T. Electrical properties of epoxy/POSS composites with homogeneous nanostructure. *IEEE Trans. Dielectr. Electr. Insul.* **2014**, *21*, 1516–1528. [[CrossRef](#)]
19. Jähren, S.; Männle, F.; Graff, J.M.; Olafsen, K. The effect of hybrid nanoparticle additives on epoxy-nanocomposite behavior and morphology. *J. Appl. Polym. Sci.* **2011**, *120*, 3212–3216. [[CrossRef](#)]
20. Fu, B.X.; Namani, M.; Lee, A. Influence of phenyl-trisilanol polyhedral silsesquioxane on properties of epoxy network glasses. *Polymer* **2003**, *44*, 7739–7747. [[CrossRef](#)]
21. Zhang, W.; Li, X.; Yang, R. Blowing-out effect and temperature profile in condensed phase in flame retarding epoxy resins by phosphorus-containing oligomeric silsesquioxane. *Polym. Adv. Technol.* **2013**, *24*, 951–961. [[CrossRef](#)]
22. Anoop, V.; Sankaraiyah, S.; Jaisankar, S.N.; Chakraborty, S.; Mary, N.L. Enhanced mechanical, thermal and adhesion properties of polysilsesquioxane spheres reinforced epoxy nanocomposite adhesives. *J. Adhes.* **2019**, *97*, 1–18. [[CrossRef](#)]
23. Bahrami, Z.; Akbari, A.; Eftekhari-Sis, B. Double network hydrogel of sodium alginate/polyacrylamide cross-linked with POSS: Swelling, dye removal and mechanical properties. *Int. J. Biol. Macromol.* **2019**, *129*, 187–197. [[CrossRef](#)]
24. Wahab, M.A.; Kim, I.; Ha, C.-S. Microstructure and properties of polyimide/poly(vinylsilsesquioxane) hybrid composite films. *Polymer* **2003**, *44*, 4705–4713. [[CrossRef](#)]
25. Anh, T.T.; Fréchette, M.; David, É.; Veillette, R.; Moraille, P. Effect of POSS-grafted titanium dioxide on the electrical and thermal properties of LDPE/TiO<sub>2</sub> polymer nanocomposite. *J. Appl. Polym. Sci.* **2017**, *135*, 46095. [[CrossRef](#)]
26. Zazoum, B.; Frechette, M.; David, E. Effect of POSS as compatibilizing agent on structure and dielectric response of LDPE/TiO<sub>2</sub> nanocomposites. In Proceedings of the 2015 IEEE Conference on Electrical Insulation and Dielectric Phenomena (CEIDP), Ann Arbor, MI, USA, 18–21 October 2015. [[CrossRef](#)]
27. Li, X.; Mao, H.; Liu, Y.; Nie, M.; Wang, Q. Compatibilization of polyhedral oligomeric silsesquioxane for polypropylene-titanium dioxide composites and effect of the processing temperature. *J. Appl. Polym. Sci.* **2017**, *134*, 44766. [[CrossRef](#)]
28. Wheeler, P.A.; Misra, R.; Cook, R.D.; Morgan, S.E. Polyhedral oligomeric silsesquioxane trisilanols as dispersants for titanium oxide nanopowder. *J. Appl. Polym. Sci.* **2008**, *108*, 2503–2508. [[CrossRef](#)]
29. Peng, D.; Qin, W.; Wu, X. Improvement of the atomic oxygen resistance of carbon fiber-reinforced cyanate ester composites modified by POSS-graphene-TiO<sub>2</sub>. *Polym. Degrad. Stab.* **2016**, *133*, 211–218. [[CrossRef](#)]
30. Dias Filho, N.L.; De Aquino, H.A.; Pires, G.; Caetano, L. Relationship between the Dielectric and Mechanical Properties and the Ratio of Epoxy Resin to Hardener of the Hybrid Thermosetting Polymers. *J. Braz. Chem. Soc.* **2006**, *17*, 533–541. [[CrossRef](#)]
31. Ye, M.; Wu, Y.; Zhang, W.; Yang, R. Synthesis of incompletely caged silsesquioxane (T7-POSS) compounds via a versatile three-step approach. *Res. Chem. Intermed.* **2018**, *44*, 4277–4294. [[CrossRef](#)]
32. Xu, Y.; Ma, Y.; Deng, Y.; Yang, C.; Chen, J.; Dai, L. Morphology and thermal properties of organic-inorganic hybrid material involving monofunctional-anhydride POSS and epoxy resin. *Mater. Chem. Phys.* **2011**, *125*, 174–183. [[CrossRef](#)]
33. Brzakałski, D.; Przekop, R.E.; Dobrosielska, M.; Sztorch, B.; Marciniak, P.; Marciniak, B. Highly bulky spherosilicates as functional additives for polyethylene processing—Influence on mechanical and thermal properties. *Polym. Compos.* **2020**, *41*, 3389–3402. [[CrossRef](#)]
34. Leito, I.; Herodes, K.; Huopolaainen, M.; Virro, K.; Künnapas, A.; Kruve, A.; Tanner, R. Towards the electrospray ionization mass spectrometry ionization efficiency scale of organic compounds. *Rapid Commun. Mass Spectrom.* **2008**, *22*, 379–384. [[CrossRef](#)] [[PubMed](#)]
35. Cech, N.B.; Enke, C.G. Practical implications of some recent studies in electrospray ionization fundamentals. *Mass Spectrom. Rev.* **2001**, *20*, 362–387. [[CrossRef](#)] [[PubMed](#)]
36. Przekop, R.E.; Jakubowska, P.; Sztorch, B.; Kozera, R.; Dydek, K.; Jałbrzykowski, M.; Osiecki, T.; Marciniak, P.; Martyła, A.; Kloziński, A.; et al. Opoka—Sediment Rock as New Type of Hybrid Mineral Filler for Polymer Composites. *AppliedChem* **2021**, *1*, 90–110. [[CrossRef](#)]

37. Kochkar, H.; Figueras, F. Synthesis of Hydrophobic TiO<sub>2</sub>–SiO<sub>2</sub> Mixed Oxides for the Epoxidation of Cyclohexene. *J. Catal.* **1997**, *171*, 420–430. [[CrossRef](#)]
38. Nguyen, V.G.; Thai, H.; Mai, D.H.; Tran, H.T.; Tran, D.L.; Vu, M.T. Effect of titanium dioxide on the properties of polyethylene/TiO<sub>2</sub> nanocomposites. *Compos. Part B Eng.* **2013**, *45*, 1192–1198. [[CrossRef](#)]
39. Tuan, V.M.; Jeong, D.W.; Yoon, H.J.; Kang, S.; Vu Giang, N.; Hoang, T.; Thinh, T.I.; Kim, M.Y. Using Rutile TiO<sub>2</sub> Nanoparticles Reinforcing High Density Polyethylene Resin. *Int. J. Polym. Sci.* **2014**, *2014*, 758351. [[CrossRef](#)]
40. Dobrosielska, M.; Dobrucka, R.; Gloc, M.; Brząkalski, D.; Szymański, M.; Kurzydłowski, K.J.; Przekop, R.E. A New Method of Diatomaceous Earth Fractionation—A Bio-Raw Material Source for Epoxy-Based Composites. *Materials* **2021**, *14*, 1663. [[CrossRef](#)]
41. Yamini, S.; Young, R.J. Stability of crack propagation in epoxy resins. *Polymer* **1977**, *18*, 1075–1080. [[CrossRef](#)]
42. Dobrosielska, M.; Dobrucka, R.; Brząkalski, D.; Gloc, M.; Rebiś, J.; Głowacka, J.; Kurzydłowski, K.J.; Przekop, R.E. Methodological Aspects of Obtaining and Characterizing Composites Based on Biogenic Diatomaceous Silica and Epoxy Resins. *Materials* **2021**, *14*, 4607. [[CrossRef](#)] [[PubMed](#)]
43. Mayes, A.M. Softer at the boundary. *Nat. Mater.* **2005**, *4*, 651–652. [[CrossRef](#)]
44. Bansal, A.; Yang, H.; Li, C.; Cho, K.; Benicewicz, B.C.; Kumar, S.K.; Schadler, L.S. Quantitative equivalence between polymer nanocomposites and thin polymer films. *Nat. Mater.* **2005**, *4*, 693–698. [[CrossRef](#)] [[PubMed](#)]
45. Ash, B.J.; Schadler, L.S.; Siegel, R.W. Glass transition behavior of alumina/polymethylmethacrylate nanocomposites. *Mater. Lett.* **2002**, *55*, 83–87. [[CrossRef](#)]